Dalton Transactions

RSCPublishing

ARTICLE

# Synthesis and Characterisation of First Row Transition Metal Complexes of Functionalized 1,2,4-Benzothiadiazines

Cite this: DOI: 10.1039/xoxxoooooox

Received ooth January 2012,
Accepted ooth January 2012

DOI: 10.1039/xoxxoooooox

www.rsc.org/

Ewan R. Clark,*[a] M. Usman Anwar,[b] Bryce J. Leontowicz,[b] Yassine Beldjoudi,[b] John J. Hayward,[b] Wesley T. K. Chan,[c] Emma L. Gavey,[d] Melanie Pilkington,[d] Eli Zysman-Colman[e] and Jeremy M. Rawson.*[a,b]

Reaction of the novel ligand 3-(2′-pyridyl)-benzo-1,2,4-thiadiazine (**L**) with the transition metal chloride salts $MCl_2 \cdot xH_2O$ ($M^{II}$ = Mn, Fe, Co, Cu and Zn) in a 2:1 mole ratio afforded the mononuclear octahedral (high spin) complexes $L_2MCl_2$ (**1a** – **1e** respectively) in which **L** binds in a chelate fashion *via* N(2) and the pyridyl N atoms. In the case of $CuCl_2$ the intermediate 1:1 four-coordinate complex $LCuCl_2$ (**2**) was also isolated which adopts a polymeric structure with pseudo-square planar molecules linked via long Cu···S contacts ($d_{Cu\cdots S}$ = 2.938(1) Å) in the apical position. In the presence of non-interacting ions, 3:1 complexes are isolated, exemplified by the reaction of **L** with $Fe(CF_3SO_3)_2$ in a 3:1 ratio which affords the low spin complex $[L_3Fe][CF_3SO_3]_2$ (**3**). Reaction of **L** with $VCl_3$ in a 2:1 mole ratio under aerobic conditions afforded the vanadyl complex $[L_2V(=O)Cl][Cl]$ (**4**).

## Introduction

Polydentate N-donor ligands continue to attract considerable attention in the field of supramolecular chemistry due to their highly predictable coordination chemistry and ease of functionalization. Ligands such as 2,2′-bipyridine,[1] phenanthroline,[2] Ar-BIAN[3] and terpyridine[4] as well as larger macrocyclic ligands such as phthalocyanines and porphyrins[5] are often found to be non-innocent ligands, revealing some potential to be involved in redox reactions.[6] Other heterocyclic N-donors such as tris(pyrazolyl) borates[7] tris(pyridyl) tripodal ligands and their heavier *p*-block bridgehead analogues[8] act as scorpionate ligands,[9] whereas heavier transition metal complexes of 2,2′-bipyridine and its derivatives, e.g. $[Ru(bipy)_3]^{2+}$, are used in light-harvesting and light emitting devices.[10] The development of polydentate N-donor ligand sets with tuneable coordination chemistry is therefore highly desirable for the construction of new functional materials. These ligands have also found applications in the emerging field of molecular magnetism since they offer a medium strength ligand field such that, for first row transition metal complexes, the magnitude of Δ is comparable with the inter-electron repulsion term (P) leading to the potential for spin-crossover behaviour in their electronic properties, i.e. for $d^4$ – $d^7$ configurations the energies of the low spin and high spin electronic configurations are comparable.[11] The development of polydentate N-donor ligand sets with tuneable coordination chemistry is therefore highly desirable for the construction of new functional materials. There has also been considerable interest in the synthesis and solid state properties of organic radicals as precursors to new electronic, optical and/or magnetic materials with interesting properties[12] In this context, new classes of magnetic materials are also becoming increasingly important as technology advances towards the miniaturization of devices. One approach to promote efficient communication between metal ions is to use a radical coupling unit, the so-called metal-radical approach, in which an organic radical ligand has been used to mediate the magnetic coupling between paramagnetic metal centres.[13] Currently the most-common families of open-shell ligands whose coordination chemistries have been exploited include semi-quinones,[14] nitroxides,[15] thiazyl radicals,[16] and verdazyls.[17] The two most common strategies employed to prepare radical complexes are: (i) coordination of the radical precursor to the desired transition metal centre first followed by a chemical/electrochemical oxidation or reduction reaction to afford the desired radical complex, and (ii) the synthesis and characterisation of the radical ligand first and subsequent coordination to the appropriate metal ion. The key to the success of both strategies is the development of efficient synthetic methodologies to both the radical ligands and their air stable precursors. Structural studies of the coordination complexes of radical precursors are useful since they may provide insight into the preferred coordination modes of the radical ligand and its likely crystal

field strength. Such data are important for tailoring future excursions into metal-radical coordination chemistry. Previous work has established that thiazyl-based radicals exhibit rich coordination chemistry with N-donor coordination that is prevalent for first row transition metals in common oxidation states[16,18] but show oxidative addition to metals in lower oxidation states.[19] We have recently reported the synthesis of a series of benzothiadiazine (BTDA) heterocycles (Scheme 1) with a variety of aryl, pyridyl and thiophenyl derivatives attached at the 3-position.[20] The benzothiadiazine heterocycle is known in the $S^{II}$, $S^{IV}$ and $S^{VI}$ oxidation states: Work by Kaszynski has pioneered synthetic methodologies to access the $S^{II}$ derivatives and has shown that they can undergo $1e^-$ oxidation to form stable radicals (when the benzo-fused ring is protected with chloro- or fluoro-substituents), some of which belong to a rare class of paramagnetic liquid cystals.[21] No structural reports of the $S^{IV}$ heterocycle are known and syntheses of the $S^{IV}$ system are few.[22] Conversely, the $S^{VI}$ thiadiazine ring system is well-established and is central to a range of commercial pharmaceuticals ubiquitously referred to as 'thiazide drugs' which were initially developed by Merck-Sharpe-Dohme[23] and used as diuretics and for the treatment of hypertension *inter alia*.

Our recent structural studies[20] revealed that the N(2) atom of the BTDA ring (adjacent to S) exhibited some basicity as a hydrogen-bond acceptor and the 2-pyridyl derivative **L** appeared well suited to act as an N,N′-chelate ligand in coordination chemistry. Herein we report the first examples of the coordination chemistry of **L** (Scheme 1) with selected first row transition metal ions.

**Scheme 1**. Molecular structure of 3-(2′-pyridyl)-1,2,4-benzothiadiazine (**L**) with numbering scheme

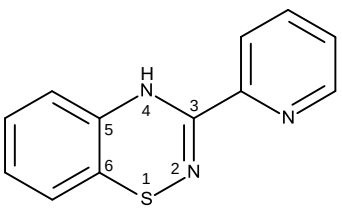


## Experimental

Ligand **L** was prepared according to the literature method in an overall yield of 65 % over 4 steps.[20] $Fe(CF_3SO_3)_2{\cdot}2CH_3CN$ was prepared according to literature procedure.[24] Solvents and other anhydrous or hydrated metal salts were obtained from commercial suppliers and used without further purification.

### Physical Measurements.

NMR spectra were recorded on a Bruker DPX300 UltraShield 300 MHz spectrometer with a Broadband AX Probe using $CDCl_3$ ($^1H$ $\delta$ = 7.26 ppm, s) as an internal reference point relative to $Me_4Si$ ($\delta$ = 0 ppm). IR spectra were obtained using a Bruker Alpha FT-IR spectrometer equipped with a Platinum single reflection diamond ATR module. Elemental compositions were determined on a PerkinElmer 2400 Series II Elemental Analyzer. UV/vis spectra were measured on a Agilent 8453 Spectrophotometer using *ca.* $1 \times 10^{-5}$ M solutions in methanol or acetonitrile in the range 200 – 800 nm. The EPR spectrum of **1c** was recorded as a polycrystalline powder at 4.2 K on a Bruker ELEXYS E580 Q-band EPR spectrometer at 5 K. EPR spectra of complex (**1e**) was recorded on a Bruker ER 200D X-band EPR spectrometer at room temperature and at 77 K using a liquid nitrogen dewar insert, whilst the EPR spectra of (**2**) and (**4**) were measured on a Bruker EMXplus X-band EPR spectrometer at room temperature. Simulations of the EPR spectra of (**1c**) and (**4**) were made using PIP via the PIP4WIN interface.[25] Variable temperature magnetic data (2–300 K) on (**1b**), (**1c**), (**2**) and (**3**) were obtained using a Quantum Design MPMS5S SQUID magnetometer using a magnetic field strength of 0.1 T. Background corrections for the sample holder assembly and sample diamagnetism (Pascal's constants) were applied.

**Preparation of $L_2MnCl_2$ (1a):** Ligand **L** (0.050 g, 0.22 mmol) and anhydrous $MnCl_2$ (0.01 g, 0.08 mmol) were stirred together in MeOH (10 mL) for 10 min at room temperature. The solution was then filtered and the filtrate left undisturbed. Red, slightly hygroscopic, crystals of (**1a**) (0.02 g, 43 %) suitable for X-ray diffraction were obtained over 24 hr. UV-Vis (MeOH): $\lambda_{max}$ nm ($\varepsilon$, $M^{-1}$ $cm^{-1}$): 201 (33100), 217 (21300), 230 (20300), 270 (32600), 325 (5300). IR ($\nu_{max}/cm^{-1}$): 3233 (w), 3195 (w), 1615 (w), 1604 (m), 1588 (m), 1563 (m), 1557 (s), 1463 (s), 1429 (s), 1326 (m), 1311 (m), 1240 (m), 1168 (m), 1125 (m), 1031 (w), 1011 (s), 934 (w), 845 (w), 792 (s), 776 (s), 748 (s), 608 (m), 581 (m), 532 (m), 461 (w). Elemental Analysis (%): Calcd for $(C_{12}H_9N_3S)_2MnCl_2{\cdot}H_2O$: C, 48.17; H, 3.37; N, 14.04. Found: C, 47.94; H, 3.09; N, 13.76.

**Preparation of $L_2FeCl_2$ (1b):** Ligand **L** (0.095 g, 0.80 mmol) and $FeCl_2{\cdot}4H_2O$ (0.040 g, 0.040 mmol) were stirred together in MeOH (10 mL) for 10 min at room temperature. The solution was then filtered and the filtrate was left undisturbed to afford red crystals (0.09 g, 77 %) of (**1b**) suitable for X-ray diffraction over 24 h. UV-Vis (MeOH): $\lambda_{max}$ nm ($\varepsilon$, $M^{-1}$ $cm^{-1}$): 201 (33100), 218 (22100), 230 (20800), 270 (28900). IR ($\nu_{max}/cm^{-1}$): 3224 (w), 3187 (w), 3043 (w), 1615 (w), 1605 (m), 1588 (m), 1537 (s), 1463 (s), 1430 (s), 1330 (s), 1330 (w), 1310 (m), 1256 (m), 1241 (m), 1167 (m), 1126 (w), 1099 (m), 1054 (w), 1030 (w), 1012 (m), 975 (w), 934 (m), 846 (m), 791 (s), 778 (w), 749 (s), 618 (m), 531 (w), 462 (m). Elemental Analysis (%): Calcd for $(C_{12}H_9N_3S)_2FeCl_2{\cdot}0.5H_2O$: C, 48.83; H, 3.24; N, 14.24. Found: C, 49.14; H, 3.36; N, 13.93.

**Preparation of $L_2CoCl_2$ (1c):** Ligand **L** (0.20 g, 0.88 mmol) was added to a solution of anhydrous $CoCl_2$ (0.10 g, 0.42 mmol) in MeOH (20 mL) and immediately sealed and left undisturbed at room temperature. Dark red, slightly hygroscopic, crystals of (**1c**) (0.210 g, 86 %) which were suitable for X-ray diffraction formed over one week. UV-Vis

 This journal is © The Royal Society of Chemistry 2014

(MeOH); $\lambda_{max}$ nm (ε, $M^{-1}$ $cm^{-1}$): 206 (30500), 233 (22600), 270 (24400), 323 (8400). IR ($\nu_{max}/cm^{-1}$): 3223 (w), 3183 (w), 1616 (w), 1606 (m), 1589 (m), 1553 (m), 1532 (s), 1464 (s), 1432 (s), 1332 (w), 1309 (m), 1257 (m), 1241 (m), 1257 (m), 1241 (m), 1167 (m), 1126 (w), 1103 (w), 1015 (w), 937 (m), 911 (m), 847 (w), 791 (s), 755 (s), 628 (m), 622 (m), 581 (w), 464 (w). Elemental Analysis (%): Calcd for $(C_{12}H_9N_3S)_2CoCl_2 \cdot 0.5H_2O$: C, 48.58; H, 3.23; N, 14.16. Found: C, 48.80; H, 3.20; N, 13.90.

**Preparation of $L_2ZnCl_2$ (1e):** Ligand **L** (0.035 g, 0.15 mmol) and anhydrous $ZnCl_2$ (0.01 g, 0.073 mmol) were stirred together in MeOH (10 mL) for 10 min at room temperature. The solution was then filtered and the filtrate was left undisturbed. Red crystals (0.010 g, 25 %) of **1e** suitable for X-ray diffraction formed over 24 hours. UV-Vis (MeOH); nm (ε, $M^{-1}$ $cm^{-1}$): 201 (39800), 215 (26000), 231 (26000), 270 (42100), 325 (4800). IR ($\nu_{max}/cm^{-1}$): 3223 (w), 3121 (w), 1619 (m), 1605 (m), 1568 (m), 1532 (w) , 1464 (s) , 1430 (s), 1329 (w), 1311 (m), 1257 (m), 1241 (m), 1168 (s), 1125 (m), 1102 (m), 1055 (m), 1015 (s), 935 (m), 791 (s), 749 (s), 613 )m), 531 (w). Elemental Analysis (%): Calcd for $(C_{12}H_9N_3S)_2ZnCl_2$: C, 48.79; H, 3.07; N, 14.22. Found: C, 48.07; H, 3.08; N, 13.79.

**Preparation of $L_2CuCl_2$ (1d) and $LCuCl_2$ (2):** Ligand **L** (180 mg, 0.079 mmol) was added to a solution of $CuCl_2 \cdot 2H_2O$ (0.102 g, 0.42 mmol) in degassed MeOH (20 mL) and the system sealed. An immediate deep red solution formed from which red-black needle-shaped crystals suitable for single crystal XRD grew slowly over one week. These were isolated by filtration and washed with MeOH (10 mL) and hexane (10 mL) before being dried *in vacuo*. The two crystalline morphologies were separated manually for X-ray diffraction studies. The major product was **2**, irrespective of **L**:$CuCl_2$ ratio, but a small number of crystals of **1d** suitable for X-ray diffraction were identified. Yield (0.20 g, 92 % based on **2**), IR ($\nu_{max}/cm^{-1}$): 3226 (w), 1603 (m), 1587 (w), 1551 (m), 1522 (s), 1468 (s), 1431 (s), 1334 (m), 1255 (m), 1128 (m), 1083 (m), 1052 (w), 1018 (m), 968 (br), 930 (w), 895 (br), 864 (w), 832 (m), 155 (s), 138 (s), 672 (m), 620 (m), 556 (m), 535 (m), 477 (m), 430 (m). Elemental Analysis (%): Calcd for $(C_{12}H_9N_3S)CuCl_2$ C, 39.84; H, 2.51; N, 11.62. Found: C, 41.45; H, 2.89; N, 11.98; UV-Vis (MeOH); nm (ε, $M^{-1}$ $cm^{-1}$): 203 (72853), 218 (33755) 277 (18002), 333 (16830).

**Preparation of $[L_3Fe][CF_3SO_3]_2$ (3):** Ligand **L** (0.050 g, 0.22 mmol) and $Fe(CF_3SO_3)_2 \cdot 2CH_3CN$ (0.048 g, 0.11 mmol) were stirred together in MeCN (15 mL) for 10 min at room temperature. The solution was then filtered and the filtrate was layered with diethyl ether. Dark purple crystals formed over one week (Yield: 0.02 g, 18 %). UV-Vis (MeCN); nm (ε, $M^{-1}$ $cm^{-1}$): 201 (42600), 218 (28700), 230 (28400), 270 (43800). IR ($\nu_{max}/cm^{-1}$) 3352 (w), 2956 (w) , 1609 (m), 1590 (w), 1569 (w), 1534 (s) , 1465 (s), 1435 (s), 1381 (m), 1366 (m), 1341 (w), 1282 (s), 1222 (s), 1166 (w), 1023 (s), 934 (w), 894 (w), 852 (w), 783 (m), 747 (s), 635 (s), 572 (m), 513 (s). Elemental Analysis (%): Calcd for $[(C_{12}H_9N_3S)_3Fe][CF_3SO_3]_2$: C, 44.06; H, 2.63; N, 12.17. Found: C, 43.48; H, 2.75; N, 12.04.

**Preparation of $[L_2VOCl][Cl] \cdot MeOH$ (4):** Ligand **L** (0.050 g, 0.22 mmol) and $VCl_3 \cdot THF$ (0.015 g, 0.04 mmol) were stirred together in a mixture of MeOH and THF (7 mL each) for 15 min at room temperature in aerobic conditions. The solution was then filtered and the filtrate was left undisturbed. Dark brown crystals formed after one week (Yield: 0.02 g 77 %). UV-Vis (MeOH); nm (ε, $M^{-1}$ $cm^{-1}$): 202 (41900), 218 (30000), 229 (37900), 270 (28400). IR ($\nu_{max}/cm^{-1}$) : 3361 (w), 1605 (m), 1588 (m), 1552 (m), 1530 (s), 1467 (s), 1434 (s), 1311 (m), 1260 (m), 1117 (m), 1061 (w), 1031 (s), 1023 (s), 972 (s), 935 (m), 898 (w), 768 (s), 744 (s), 692 (m), 675 (m), 578 (m), 526 (w), 516 (w), 480 (s), 460 (m), 432 (m), 421 (m). Elemental Analysis (%): Calcd for $[(C_{12}H_9N_3S)_2VOCl_2][Cl] \cdot MeOH$: C, 48.08; H, 3.55; N, 13.46. Found: C, 48.04; H, 3.45; N, 13.37.

**X-Ray Crystallography**

Crystals of (**1c**), (**1d**) and (**2**) were mounted on a glass fibre with fluoropolymer and examined on a Nonius Kappa diffractometer equipped with a CCD area detector and an Oxford Cryostream cooler at 180(2) K using graphite-monochromated Mo-Kα radiation (λ = 0.71073 Å). Data were collected using COLLECT[26] and the final cell constants determined from full least squares refinement of all reflections using SCALEPACK.[27] Data were reduced and processed and an absorption correction applied using HKL, DENZO and SCALEPACK. Structures were initially solved using SIR-92[28] and subsequently refined against $F^2$ within the SHELXTL suite.[29] All non-H atoms were refined anisotropically and H atoms added at calculated positions and refined using a riding model.

Crystals of (**1a**), (**1b**), (**1e**), (**3**) and (**4**) were mounted on a cryoloop with paratone oil and examined on a Bruker APEX diffractometer equipped with CCD area detector and Oxford Cryostream cooler at 150(2) K using graphite-monochromated Mo-Kα radiation (λ = 0.71073 Å). Data were collected using the APEX-II software,[30] integrated using SAINT[31] and corrected for absorption using a multi-scan approach (SADABS).[32] Final cell constants were determined from full least squares refinement of all observed reflections. The structures were solved by direct methods (SHELXS within SHELXTL)[29] to reveal most non-H atoms. Remaining atom positions were located in subsequence difference maps and the structure refined with full least squares refinement on $F^2$ within the SHELXTL suite.[29] Hydrogen atoms were placed at calculated positions and refined isotropically with a riding model.

In some cases the anisotropic displacement parameters of the S atoms appeared significantly elongated consistent with some dynamic or static disorder of the thiadiazine ring and the S atom was refined over two or more positions. In the case of (**3**) both of the two crystallographically independent triflate ions were disordered and modelled over two sites. Crystallographic data for (**1** – **4**) are summarized in Table 1. The structures have been deposited with the CCDC (deposition numbers CCD 1002532-1002539).

Table 1 Crystal data for complexes **1** – **4**.

| | **1a** | **1b** | **1c** | **1d** |
|---|---|---|---|---|
| Formula | $C_{24}H_{18}N_6S_2MnCl_2$ | $C_{24}H_{18}N_6S_2FeCl_2$ | $C_{24}H_{18}N_6S_2CoCl_2$ | $C_{24}H_{18}N_6S_2CuCl_2$ |
| FW | 580.40 | 581.31 | 584.39 | 589.00 |
| Temp. (K) | 150(2) | 150(2) | 180(2) | 180(2) |
| Crystal system | Orthorhombic | Orthorhombic | Orthorhombic | Orthorhombic |
| Space group | *Pbcn* | *Pbcn* | *Pbcn* | *Pca2₁* |
| *a*/Å | 13.468(6) | 13.3122(16) | 13.294(3) | 9.8897(2) |
| *b*/Å | 9.758(4) | 9.8775(12) | 9.846(2) | 13.1801(4) |
| *c*/Å | 18.440(8) | 18.354(2) | 18.407(4) | 18.5634(6) |
| α/° | 90.00 | 90.00 | 90.00 | 90 |
| β/° | 90.00 | 90.00 | 90.00 | 90 |
| γ/° | 90.00 | 90.00 | 90.00 | 90 |
| *V*/Å$^3$ | 2423.3(17) | 2413.4(5) | 2409.2(8) | 2419.69(12) |
| *Z* | 4 | 4 | 4 | 4 |
| $D_{c/Mg\ m^{-3}}$ | 1.591 | 1.60 | 1.611 | 1.617 |
| μ(MoKα)/ cm$^{-1}$ | 0.965 | 1.047 | 1.135 | 1.323 |
| Total reflns | 2803 | 2764 | 2118 | 2544 |
| Reflns [I>2σ(I)] | 2375 | 2434 | 1383 | 2244 |
| $R_{int}$ | 0.0361 | 0.0174 | 0.0655 | 0.062 |
| $R_1$[a], $wR_2$[b] | 0.046, 0.095 | 0.041, 0.113 | 0.056, 0.154 | 0.039, 0.094 |
| $e^-$ (min/max) | +0.38/-0.32 | +1.00/-0.50 | +0.43/-0.43 | +0.67/-0.53 |

| | **1e** | **2** | **3** | **4** |
|---|---|---|---|---|
| Formula | $C_{24}H_{18}N_6S_2ZnCl_2$ | $C_{12}H_9N_3SCuCl_2$ | $C_{38}H_{27}F_6FeN_9O_6S_5$ | $C_{24}H_{18}N_6S_2VOCl_2$ |
| FW | 590.83 | 361.72 | 1035.83 | 643.90 |
| Temp. (K) | 150(2) | 180(2) | 150(2) | 150(2) |
| Crystal system | Orthorhombic | Monoclinic | Triclinic | Monoclinic |
| Space group | *Pbcn* | *Cc* | *P-1* | *P2₁/n* |
| *a*/Å | 13.282(7) | 9.0429(3) | 12.236(4) | 12.606(6) |
| *b*/Å | 9.799(5) | 22.3081(5) | 14.022(4) | 12.609(6) |
| *c*/Å | 18.426(10) | 7.1341(3) | 15.179(5) | 17.194(8) |
| α/° | 90.00 | 90.00 | 88.805(3) | 90.00 |
| β/° | 90.00 | 116.720(3) | 79.225(3) | 96.886(5) |
| γ/° | 90.00 | 90.00 | 73.710(3) | 90.00 |
| *V*/Å$^3$ | 2398(2) | 1285.48(8) | 2454.4(13) | 2713(2) |
| *Z* | 4 | 4 | 2 | 4 |
| $D_{c/Mg\ m^{-3}}$ | 1.637 | 1.869 | 1.402 | 1.576 |
| μ(Mo-Kα)/ cm$^{-1}$ | 1.449 | 2.262 | 0.594 | 0.752 |
| Total reflns | 2735 | 2593 | 10986 | 4773 |
| Reflns [*I*>2σ(*I*)] | 2283 | 2448 | 8880 | 3609 |
| $R_{int}$ | 0.0387 | 0.0419 | 0.0475 | 0.0528 |
| $R_1$[a], $wR_2$[b] | 0.036, 0.078 | 0.032, 0.066 | 0.067, 0.186 | 0.077, 0.214 |
| $e^-$ (min/max) | +0.39/-0.30 | +0.34/-0.43 | +1.70/-0.84 | +2.04/-1.47 |

[a] ($I > 2\sigma(I)$), [b] (all data)

**Density Functional Theory (DFT) Calculations.**

All calculations were performed with the Gaussian 09 suite.[33] The level of theory for all DFT calculations[34] was B3LYP.[35] The 6-31G* basis set[36] was used for N directly linked to copper while the other atoms where undertaken with 3-21G*basis set,[37] and the VDZ (valence double ζ) with SBKJC effective core potential basis set[37a,38] was used for copper.

## Results and Discussion

Ligand **L** was prepared as red needles according to the literature method from commercial starting materials in good yield (65%) over 4 steps.[20] Reaction of **L** with the corresponding divalent metal chloride salt in either MeOH or MeCN in a 2:1 molar ratio at ambient temperature afforded the complexes $L_2MCl_2$ (M = Mn (**1a**), Fe (**1b**), Co (**1c**), Cu (**1d**) and Zn (**1e**)). Crystals suitable for X-ray diffraction were grown by storage of saturated solutions of **1** over periods between 24h and 1 week. These crystals proved slightly hygroscopic, absorbing small quantities of water upon standing in the open atmosphere but otherwise appeared air stable. The UV/Vis spectra of **1a - 1e** are dominated by a series of intense ($\varepsilon = 10^3 - 10^5$ M$^{-1}$cm$^{-1}$) π–π* ligand-centered absorption bands at 201, 217, 230, 257, and 270 nm (see supplementary, Fig S1†). There are additionally two lower intensity absorption bands at 330

and 420 nm that are attributed to intra-ligand charge transfer transitions. These assignments are corroborated by the fact that the absorption profiles for the complexes match the absorption spectrum of the free ligand. Indeed, the absorption profiles are insensitive to the nature of the *d*-block metal ion and exhibit a negligible effect on the position of these bands, though some differences in relative intensity are evident. Thus, even high spin $d^5$ $Mn^{2+}$ and $d^{10}$ $Zn^{2+}$ complexes of this ligand appear red.

The structures of (**1a** – **1c**) and (**1e**) (M = Mn, Fe, Co and Zn) were found to be isomorphous, crystallising in the orthorhombic space group *Pbcn* with half a unique molecule in the asymmetric unit, whereas the $Cu^{II}$ analogue crystallised in the orthorhombic space group $Pca2_1$ with $Z' = 1$. In the latter case the nature of the Jahn-Teller distortion (*vide infra*) leads to an inequivalence in Cu-Cl and Cu-N bond lengths, lowering the crystallographic symmetry but, in other respects, the structure and packing of (**1d**) is the same as the other derivatives. In all cases the metal centre adopts a pseudo-octahedral geometry with the two chloride ligands mutually *cis*, and the benzothiadiazine-N atoms located *trans* to the Cl atoms (Fig. 1). The coordination geometries at the metal centre are presented in Table 2.

**Figure 1**. Molecular structure of **1c** as representative of the series (**1a** – **1e)** with thermal ellipsoids for non-H atoms drawn at the 50% probability level.

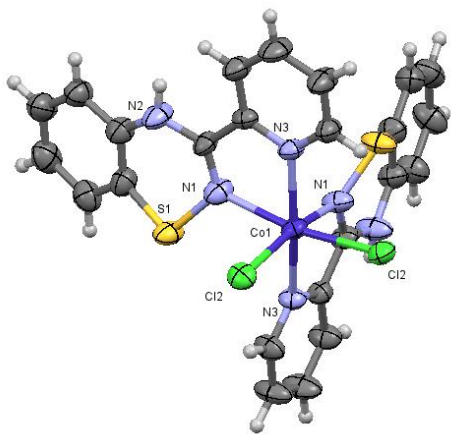


The general trend in metal-ligand bond lengths for (**1a** – **1e**) are all consistent with a (high-spin) $M^{II}$ centre with the initial decrease (M = Mn to Co) associated with increasing effective nuclear charge on traversing the first transition metal series and subsequent increase (Cu and Zn) associated with the addition of extra electrons into the $e_g$* orbitals. In the case of $Cu^{II}$, the complex exhibits a marked Jahn-Teller elongation along the N(22)Cu(1)Cl(2) axis (Table 2). The chelate ligand **L** exhibits internal $N_{BTDA}$-M-$N_{py}$ angles in the range 71.04(8) – 79.2(2)$^o$ with the largest angle associated with the Jahn-Teller elongated $Cu^{II}$ centre.

The benzothiadiazine heterocycle is formally 12π anti-aromatic and previous structural studies have revealed a folding of the $C_3N_2S$ heterocycle across the H-N···S hinge, albeit with a low energy barrier to distortion.[20] In the series (**1a** – **1e**), some minor disorder is typically observed in the S atom position such that the S atom resides above or below the $C_3N_2$ plane. In addition the N-H group exhibits a propensity to be involved in hydrogen bonding and in these complexes the N-H group forms N-H···Cl hydrogen bonds [$d_{N\cdots Cl}$ = 3.135(4) – 3.243(3) Å] between molecules. The presence of two hydrogen bond N-H donors and two hydrogen bond Cl acceptors affords a two-dimensional hydrogen-bonded grid in the *ab* plane (see supplementary, Fig S2†).

The electronic structure of the $Co^{II}$ complex was probed through SQUID magnetometry and low temperature Q-band EPR spectroscopy. The SQUID data were consistent with the presence of high spin $Co^{II}$ with residual unquenched orbital angular momentum. Above 50 K (**1c**) exhibits Curie-Weiss behaviour with $C$ = 2.394 emu.K.mol$^{-1}$ (θ = -12.3 K associated with zero field splitting effects) consistent with $S = {}^3/_2$ and g = 2.26. In the low temperature regime (T < 50 K), depopulation of the excited states arising from spin-orbit coupling occurs and the system behaves as a Kramer's doublet ($C$ = 1.614, θ = -0.46 K) consistent with weak antiferromagnetic exchange between $S_{eff}$ = ½ spins with g = 4.15 (Fig. 2). A low temperature EPR spectrum (Q-band 5 K) reveals significant anisotropy arising from spin orbit coupling ($g_1$ = 2.00, $g_2$ = 3.60, $g_3$ = 6.15) with <g> = 3.92 in agreement with the low temperature SQUID data.

**Table 2** Molecular parameters for (**1a** – **1e**)

| M | M-$N_{py}$/Å | M-$N_{BTDA}$/Å | M-Cl/Å | $N_{py}MN_{BTDA}$/$^{o1}$ | $N_{py}MN_{BTDA}$/$^{o2}$ | $N_{py}$MCl/$^o$ | $N_{BTDA}$MCl/$^o$ | ClMCl/$^o$ | N...Cl/Å |
|---|---|---|---|---|---|---|---|---|---|
| Mn | 2.260(2) | 2.268(2) | 2.460(1) | 71.04(8) | 96.23(8) | 92.85(6) | 89.27(7) | 95.42(5) | 3.243(3) |
| | | | | | | 99.03(6) | 163.77(5) | | |
| Fe | 2.180(2) | 2.194(2) | 2.4285(7) | 73.74(7) | 94.69(7) | 93.38(5) | 89.79(6) | 92.98(3) | 3.227(2) |
| | | | | | | 97.73(5) | 167.09(5) | | |
| Co | 2.145(4) | 2.142(4) | 2.418(2) | 75.3(2) | 96.7(2) | 93.0(1) | 89.09(1) | 92.42(8) | 3.224(6) |
| | | | | | | 94.9(1) | 168.2(1) | | |
| Cu | 2.033(5) | 2.038(5) | 2.327(2) | 79.2(2) | 95.8(2) | 93.5(1) | 85.1(1) | 89.16(9) | 3.135(4) |
| | 2.040(4) | 2.288(5) | 2.758(2) | 75.6(2) | 94.9(2) | 95.3(1) | 93.3(1) | | 3.224(5) |
| | | | | | | 93.3(1) | 168.7(1) | | |
| | | | | | | 93.1(1) | 170.2(1) | | |
| Zn | 2.158(2) | 2.206(2) | 2.409(1) | 74.06(7) | 94.39(7) | 93.42(5) | 89.14(6) | 94.19(5) | 3.222(3) |
| | | | | | | 97.56(6) | 167.38(5) | | |

[1] angle within the chelate ring; [2] angles between N atoms in different rings.

**Figure 2**. Curie-Weiss behaviour of $L_2CoCl_2$ (**1c**) (the circles represent experimental data, the straight lines, best fits to Curie-Weiss behaviour in high temperature and low temperature limits); (inset) the Q-band EPR spectrum of $L_2CoCl_2$ at 5 K.

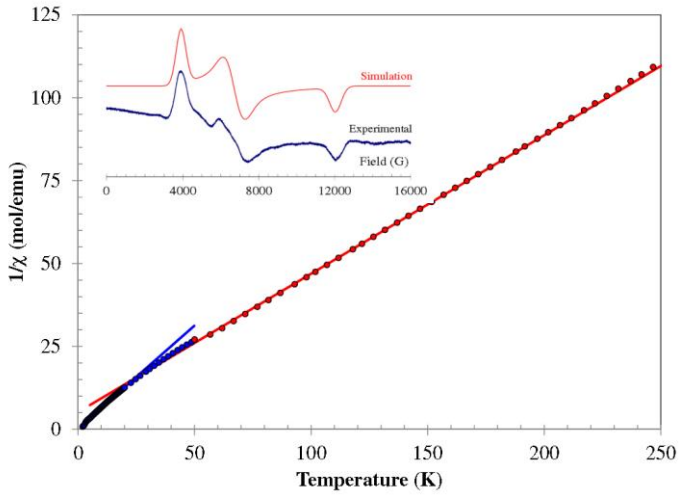


In the case of $CuCl_2$, the coordination chemistry proved more problematic and red crystals of (**1d**) could only be isolated under anaerobic conditions. In addition the 1:1 complex $[LCuCl_2]_n$ (**2**) was always formed (also as red crystals) alongside the anticipated 2:1 complex (**1d**), with (**1d**) isolated as the ***minor*** product. The ***major*** product, compound (**2**) could be isolated in reasonable purity from the 1:1 reaction of **L** with $CuCl_2{\cdot}2H_2O$ under anaerobic conditions, with only minor contamination from (**1d**) based on micro-analytical data. The stability of (**2**) may be attributable to its low solubility and polymeric nature (*vide infra*).

The 1:1 adduct (**2**) crystallises in the monoclinic space group *Cc* with a single $LCuCl_2$ fragment in the asymmetric unit. The $Cu^{II}$ centre adopts a four-coordinate $CuN_2Cl_2$ geometry, intermediate between tetrahedral and square planar, with the angles between the $CuN_2$ and $CuCl_2$ planes being 27.55° (*cf* square planar at 0° and tetrahedral at 90°). Both the Cu-N bond distances within the chelate ring (1.997(3) – 2.026(3) Å) and Cu-Cl bond lengths (2.228(1)-2.244(1) Å) are a little shorter than those in (**1d**), consistent with the lower coordination number of the $Cu^{II}$ centre. As a consequence the resultant chelate bite angle NCuN of 80.1(1)° is a little larger than those observed for (**1a-e**).

Molecules of **2** are linked together to form a one-dimensional polymeric chain parallel to the *c*-axis *via* a long axial Cu···S contact ($d_{Cu\cdots S}$ = 2.938(1) Å) affording an overall pseudo-5-coordinate geometry at the $Cu^{II}$ centre which is best described as close to square pyramidal with an Addison τ value of 0.23 (0 for square pyramidal and 1 for trigonal bipyramidal). In addition, the molecules are linked *via* a single N-H···Cl hydrogen bond parallel to the *a*-axis (N···Cl 3.233(3) Å). The combination of Cu···S and N-H···Cl contacts likely contribute significantly to the low solubility of (**2**). The observation of Cu···S contacts in (**2**) is in stark contrast to the other metals in this study and reflects the softer nature of copper.

Solid state EPR studies on (**2**) reveal an axial spectrum (see supplementary, Fig.S3†) with $g_{\|}$ = 2.200 and $g_{\perp}$ = 2.054 (<g> = 2.103) consistent with a metal-based electron. The pattern of g-values ($g_{\|} > g_{\perp} > g_e$) reflect those expected for an unpaired electron of $d_{x^2-y^2}$ character, in agreement with a pseudo-square planar geometry.

**Figure 3**. (a) Asymmetric unit of **2** with thermal ellipsoids for non-H atoms drawn at the 50 % probability level; (b) supramolecular chains of **2** formed via Cu···S interactions parallel to the *c* axis and (c) NH···Cl hydrogen bonding interactions in **2** parallel to *a*.

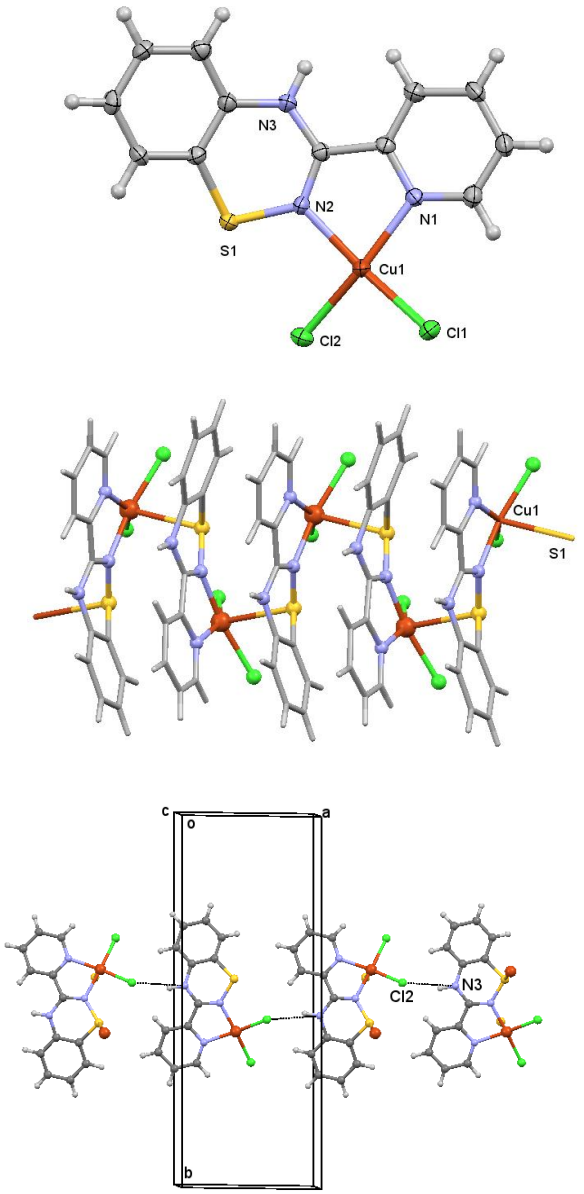


Despite the polymeric nature of (**2**) with a two atom S-N bridge between $Cu^{II}$ centres, SQUID magnetic studies (5 – 300 K) revealed (**2**) is a simple $S$ = ½ paramagnet, obeying Curie-Weiss behaviour with $C$ = 0.416 emu.K.mol$^{-1}$and θ = +1.43 K (see supplementary, Fig. S4†). The M *vs* H plot at 5 K fits the

Brillouin function for an $S$ = ½ paramagnet with g = 2.103 (see supplementary, Fig. S4†) and is similarly in agreement with simple $S$ = ½ paramagnetic behaviour. The absence of significant magnetic exchange between $Cu^{II}$ centres is consistent with a $d_{x^2-y^2}$ based unpaired electron which inhibits efficient overlap with ligands positioned along the *z*-axis.

In order to coordinate a further equivalent of **L** to the metal centre, the 3:1 complex $[L_3Fe][CF_3SO_3]_2$ (**3**) was prepared in a similar manner to the $\mathbf{L}_2MCl_2$ salts, but utilising the weakly coordinating triflate anion to offer six potential coordination sites at the $Fe^{II}$ centre. Complex (**3**) crystallises in the triclinic space group *P-1* with one unique molecule of (**3**) in the asymmetric unit. The $Fe^{II}$ centre exhibits a six-coordinate octahedral geometry with an $N_6$ donor set from three chelate ligands **L** (Fig. 4). Whilst the molecule is chiral, the presence of an inversion centre in the *P-1* space group means that the sample is a racemate, comprising both Λ and Δ forms. The Fe-N bond lengths span the range 1.957(3) – 1.970(3) Å, notably shorter than (**1b**) (2.180(2) – 2.194(2) Å) indicative of a low spin $Fe^{II}$ complex. These distances are comparable with other low spin $Fe^{II}$-N bond lengths with $FeN_6$ coordination geometries; low spin $Fe^{II}$ typically being in the region 1.95 – 2.00 Å whereas the high spin configurations have longer Fe-N distances, *ca.* 2.12 – 2.18 Å.[39]

**Figure 4**. Asymmetric unit of **3** with thermal ellipsoids for non-H atoms drawn at the 50% probability level (disorder in the triflate anions omitted for clarity).

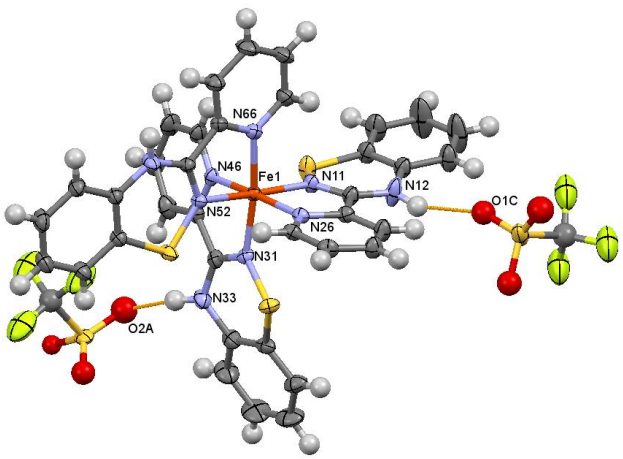


The $[FeL_3]^{2+}$ cation forms hydrogen bonds to both of the triflate anions (Fig. 4). One of the three hydrogen bond donor N-H units of the benzothiadiazine ring forms a single N-H···O-S hydrogen bond between N(12) and O(1C) ($d_{N\cdots O}$ = 2.828(7) Å) whereas the remaining two N-H bond donors hydrogen bond to the same triflate counter-ion forming a chain structure parallel to the crystallographic *a*-axis with N···O distances in the range 2.814(6) and 2.967(7) Å. The presence of hydrogen-bonding affords well-ordered $SO_3^-$ units but the corresponding $CF_3$ moieties of the two crystallographically independent triflates are each disordered over two sites. SQUID measurements on **3** revealed it was low spin throughout the temperature range from 5 K to 300 K (see ESI, Fig. S5†). The observation of high spin $FeL_2Cl_2$ but low spin $[FeL_3]^{2+}$ are consistent with the stronger ligand field imposed by **L** relative to Cl. Additional DSC studies up to 150 °C revealed no evidence for a first order phase transition expected for a low-spin to high-spin transition upon warming.

Reaction of **L** with $VCl_3$ under aerobic conditions led to metal oxidation and isolation of the vanadyl complex, $[L_2V(=O)Cl]Cl$ (**4**) as a dark brown crystalline solid rather than isolation of $[L_2VCl_2]Cl$. Confirmation of the assignment as a vanadyl ion is based on crystallographic studies, EPR and IR spectroscopies. The $\nu_{V=O}$ stretch of penta-coordinate vanadyl ions typically occurs as a strong band in the region 970 – 1000 $cm^{-1}$, with a modest shift (20 – 30 $cm^{-1}$) to lower energy for 6-coordinate complexes.[40] For (**4**) an intense absorption in the IR (972 $cm^{-1}$) was observed consistent with this V=O stretching vibration. In the solid state the EPR spectrum of (**4**) revealed a broad singlet. Its poor solubility in several solvents including THF and DMF precluded solution measurements but a thin film cast from molten *p*-$ClC_6H_4CN$ yielded an axial EPR spectrum (see supplementary, Fig. S6†) with $g_{\|}$ = 1.950 and $g_{\perp}$ = 1.994 and $a_{V(\|)}$ = 172 G and $a_{V(\perp)}$ = 66 G (<g> = 1.979 and $<a_V>$ = 101 G). The g-value is slightly less than $g_e$, typical of an ion with a less than half-filled shell and the anisotropic parameters themselves are typical of the vanadyl ion.[41]

Complex (**4**) was found to crystallise in the monoclinic space group $P2_1/n$ as a methanol solvate with one molecule in the asymmetric unit. Initial refinement as $[VL_2Cl_2]Cl$ revealed large thermal parameters for one of the coordinated Cl atoms and a corresponding unreasonably short V-Cl bond length. Improved residual electron density was obtained when it was refined as $[VOL_2Cl]Cl$ and this assignment was subsequently confirmed by IR and EPR spectroscopy (see above). The structure is shown in Figure 5. As with (**1**) and (**3**), the coordination geometry around vanadium is pseudo-octahedral with the benzothiadiazine ligands chelating the vanadyl centre with V-N bond lengths in the range 2.119(4) – 2.236(4) Å with the longest V-N bond (2.236(4) Å) *trans* to the vanadyl O atom substantially longer than the other three (mean 2.125(4) Å). The two remaining coordination sites are occupied by a chloride ion ($d_{V-Cl}$ = 2.261(2) Å) and a vanadyl oxygen ($d_{V=O}$ = 1.799(3) Å). The V=O bond length is somewhat longer than those reported elsewhere for octahedral *cis*-$VOClN_4$ complexes (1.59 – 1.72 Å) but substantially shorter than V-O single bonds in six-coordinate $VOClN_4$ $V^{III}$ complexes (2.11 Å). A bond valence sum analysis confirmed its assignment as $V^{IV}$. In addition, the observed elongation of the V-N bond *trans* to O is typical of such vanadyl complexes. The non-coordinated lattice chloride, Cl(3), is well located in the crystal lattice and hydrogen bonded to a lattice solvent methanol ($d_{Cl\cdots O}$ = 3.086(6)Å) and additionally bridging two cations *via* a pair of Cl···H-N hydrogen bonds (Cl(3)···N(12) 3.219(4) and Cl(3)···N(22) 3.154(5)Å) to the benzothiadiazine ring, leading to a hydrogen-bonded chain structure along the *ac* diagonal.

**Figure 5**. Asymmetric unit of (**4**) with thermal ellipsoids for non-H atoms drawn at the 50% probability level.

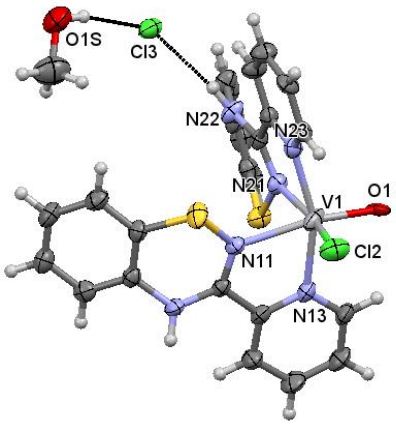


A comparison of the ligand coordination geometry with respect to the free ligand[20] indicates, as expected, that the major changes in geometry of the coordinated ligand are associated with the N-bound heteroatom of the thiadiazine ring. Specifically N-coordination leads to somewhat variable lengthening of both C-N and N-S bond lengths with C-N bond lengths in the range 1.286(8) – 1.2995(5) Å and S-N bonds in the range 1.700(4) – 1.745(6) Å (*cf* free ligand at 1.287(2) and 1.705(1) Å). This suggests some concomitant bond-weakening within the heterocycle upon coordination.

The N,N′-chelate ligand **L** offers two N donors to the metal centre; a pyridyl N-donor and the thiadiazine N-donor. Based on the M-N bond lengths within the series **1a** – **1e**, the pyridyl N atoms are consistently the same as or slightly shorter than the thiadiazine M-N bond distances (within 3 esd's), suggesting the thiadiazine ring is a slightly weaker N-donor than the pyridyl N atom. However within this series the thiadiazine ring is always bonded *trans* to π-donor Cl whereas the pyridyl N-donor atoms are mutually *trans*. An investigation of the geometry in **2** where both N atoms are *trans* to Cl, reveals the Cu-N bond to the thiadiazine ring to be marginally shorter (1.997(3) Å) than the pyridyl-N atom (2.026(3) Å). Conversely, in **3**, when all the pyridyl-N atoms are *trans* to thiadiazine-N atoms, the thiadiazine Fe-N bonds (1.957(3) – 1.970(3) Å) are identical to the pyridyl Fe-N bonds (1.959(2) – 1.966(3) Å) within error. In **4**, the benzothiadiazine-N again adopts a position *trans* to the π-donor O and Cl atoms. In this case the strong π-donor O leads to a greater lengthening of the V-N bond *trans* to it (2.236(4) Å) in relation to the V-N bond *trans* to Cl (2.129(4) Å). These bonds are, in an analogous fashion to **1a** – **1e**, longer than the pyridyl V-N bonds (2.119(4) – 2.126(4) Å) which are located mutually *trans* to each other.

These studies reveal that the novel ligand **L** possesses a strong ability to form chelate complexes with a broad cross-section of first row transition metal centres. These initial studies show, as expected, that its crystal field strength is broadly comparable with other chelate N-donor ligands such as bipy and phen. Amongst the series of complexes (**1**) (M = Mn – Zn), the Cl atoms are all located *trans* to the benzothiadiazine N(2) atom.

DFT calculations on (**1d**) were undertaken as representative of this series of complexes. These reproduce the Jahn-Teller distortion associated with (**1d**), albeit underestimating the Cu-Cl bond by 0.07 Å. An examination of the spin density distribution reveals a localization of the spin to the $d_{x^2-y^2}$ orbital of the $Cu^{II}$ ion (Fig. 6), suggesting limited acceptor character of the benzothiadiazine ring. This is unsurprising given the electron-rich nature of the thiadiazine ring. Preliminary electrochemical studies on **L** reveal irreversible oxidation, consistent with a *ec* mechanism in which $1e^-$ oxidation is coupled to a chemical process such as deprotonation of the N-H group, although work by Kaszynski has shown the benzo-fused ring is also susceptible to attack and halogenation of the benzo-ring may also be desirable.[21]

**Figure 6.** Two orientations of (**1d**) overlaid with the spin density distribution for (0.0004 iso).

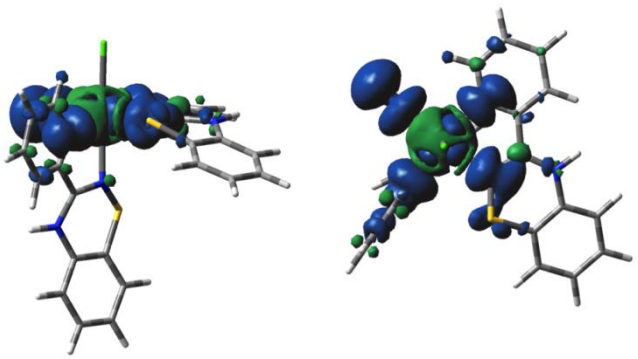

The propensity for the parent benzothiadiazine N(4)H atom to be involved in hydrogen bonding seems to extend to the transition metal complexes of this ligand, suggesting that these hydrogen-bonded frameworks can be used to construct supramolecular framework structures in which the hydrogen-bonded motif may facilitate some degree of cooperativity.

## Conclusions

The 3-(2′-pyridyl)-benzo-1,2,4-thiadiazine ligand, **L**, is shown to not only be a versatile medium field ligand in coordination chemistry but to exhibit a capacity for hydrogen bonding which may be beneficial in enhancing cooperative phenomena and generating supramolecular self-assembled structures. Further studies are underway to (i) probe the reactivity of ligand **L** with heavier second and third row metals, (ii) tune the auxiliary ligands to tailor the magnetic properties of the $Fe^{II}$ and $Co^{II}$ complexes into an appropriate region to observe spin transition behaviour and (iii) examine the redox behaviour of such complexes. Notably the reaction of $VCl_3$ with **L** under aerobic conditions leads to $1e^-$ oxidation of $V^{III}$ in preference to $1e^-$ oxidation of the benzothiadiazine ring, suggesting careful tailoring of both ligand and metal oxidation state will be required to selectively oxidize ligand **L**. Further studies to alkylate at N(4) and protect selected positions on the

 This journal is © The Royal Society of Chemistry 2014

benzothiadiazine ring are planned. Such tailoring of the oxidation states of the metal in order to modify ligand reactivity have previously been observed for the dithiadiazolyl radical, $RCNSSN^{\bullet}$ in which (i) oxidation of the radical to the cation can be observed for metals in higher oxidation states;[42] (ii) N-coordination occurs for metals in common oxidation states,[16,43] but (iii) oxidative addition to the S-S bond occurs for metals in low oxidation states.[19] In addition, the evident ability of the $S^{II}$ centre to become involved in the coordination chemistry is likely to lead to more diverse reactivity towards softer heavy transition metal centres.

## Acknowledgements

We would like to thank the EPSRC (E.R.C.), NSERC (M.P.; J.M.R.; E.Z.-C.) and the Canada Research Chairs program (M.P.; J.M.R.) for financial support as well as the CFI and ORF for equipment infrastructure grants (M.P.; J.M.R.). We would like to thank J.E. Davies (Cambridge) for data collection on selected samples in this paper, Dr A. Alberola for Q-band EPR spectra of **1c**, Prof. F. Razavi (Brock) for SQUID time to measure the magnetism of **1b** and **2** and Dr. J. Auld for microanalytical data.

## Notes and references

[a] Department of Chemistry, University of Cambridge, Lensfield Road, Cambridge CB2 1EW, UK.

[b] Department of Chemistry and Biochemistry, University of Windsor, 401 Sunset Avenue, Windsor, ON, N9B 3P4, CANADA.

[c] Laboratory of X-Ray Crystal Structure Analysis, Department of Applied Biology and Chemical Technology, Hong Kong Polytechnic University, Hung Hom, Kowloon, Hong Kong SAR.

[d] Department of Chemistry, Brock University, 500 Glenridge Avenue, St Catharines, Ontario, L2S 3A1, CANADA.

[e] EastChem School of Chemistry, University of St Andrews, North Haugh, St. Andrews, Fife, UK KY16 9ST

† Electronic Supplementary Information (ESI) available include structures of **1** – **4** in cif format, UV/Vis spectra for L and **1** – **4**, crystal packing of **1**, solid state EPR spectrum of **2**, magnetic measurements on **2** and **3**, EPR spectrum of **4** as a thin film in *p*-$ClC_6H_4CN$. See DOI: 10.1039/b000000x/

1 (a) C. Kaes, A. Katz and M. W. Hosseini, *Chem. Rev.*, 2000, **100**, 3553; (b) B.-H. Lee, M.-L. Tong and X.-M. Chen, *Coord. Chem. Rev.*, 2005, **249**, 545.

2 P. G. Sammes and G. Yahioglu, *Chem. Soc. Rev.*, 1994, **23**, 327

3 N. J. Hill, I. Vargas-Baca and A. H. Cowley, *Dalton Trans*, 2009, 240.

4 (a) H. Hofmeier and U. S. Schubert, *Chem. Soc. Rev.*, 2004, **33**, 373; (b) U. S. Schubert and C. Eschbaumer, *Angew. Chem. Int. Ed. Engl.*, 2002, **41**, 2892; (c) "Modern Teryridine Chemistry" U. S. Schubert, H. Hofmeier and G. R. Newkome, Wiley-VCH, 2006.

5 (a) C. G. Claessens, U. Hahn and T. Torres, *The Chemical Record*, 2008, **8**, 75; (b) "Functional Phthalocyanine Molecular Materials", *Structure and Bonding*, **135**. (D.M.P. Mingos Ed); (c) "Phthalocyanine Molecules: Synthesis, Structure and Function", N. B. McKeown, Cambridge University Press, 1998; (d) "The Porphyrin Handbook" (Eds. K. Kadish, R. Guilard and K. M. Smith), **11** – **20**, Academic Press, 2003.

6 (a) G. Accorsi, A. Listorti, K. Yoosaf and N. Armaroli, *Chem. Soc. Rev.*, 2009, **38**, 1690; (b) B. d. Bruin and W. A. Gal, *Inorg. Chem.*, 2001, **40**, 4649; (c) P. J. Chirik and K. Wieghardt, *Science*, 2010, **327**, 794; (d) B. d. Bruin, E. Bill, E. Bothe, T. Weyhermuller and K. Wieghardt, *Inorg. Chem.* 2000, **39**, 2936; (e) M. Schwalbe, R. Metzinger, T. S. Teets and D. G. Nocera, *Chem. Eur. J.*, 2012, **18**, 15449; (f) N. N. Adarsha and P. Dastidar, *Chem. Soc. Rev.*, 2012, **41**, 3039; (g) W. B. Schwederski, W. Kaim and B. Schwederski, *Coord. Chem. Rev.*, 2010, **254**, 1580; (h) A. B. Sorokin, *Chem. Rev.* 2013, **113**, 8152; (i) A. Vlcek. Jr., *Coord. Chem. Rev.*, 2002, **230**, 225; (j) T. Zell, P. Milko, K. L. Fillman, Y. Diskin-Posner, T. Bendikov, M. A. Iron, G. Leitus, Y. Ben-David, M. L. Neidiq and D. Milstein, *Chem. Eur. J.* 2014, DOI: 10.1002/chem.201304631

7 (a) A.L. Rheingold, R.L. Ostrander, B.S. Haggerty and S. Trofimenko, *Inorg. Chem.*, 1994, **33**, 3666; (b) S. Trofimenko, *Chem. Rev.*, 1993, **93**, 943;

8 (a) H.R. Simmonds and D.S. Wright, *Chem. Commun*, 2012, **48**, 8617 and refs therein; (b) T.H. Bullock, W.T.K. Chan, D.J. Eisler, M. Streib and D.S. Wright, *Dalton Trans.*, 2009, 1046; (c) F. Ambruster, I. Fernandez and F. Breher, *Dalton Trans.*, 2009, 5612; (d) A. Steiner and D. Stalke, *Inorg. Chem.*, 1995, **34**, 4846.

9 G. R. Owen, *Chem. Soc. Rev.*, 2012,**41**, 3535–3546.

10 E. A. Medlycott and G. S. Hanan, *Chem. Soc. Rev.*, 2005, **34**, 133.

11 (a) P. Gutlich, H.A. Goodwin (Eds.), *Spin Crossover in Transition Metal Compounds* **I**–**III**, Springer, *Top. Curr. Chem.* 2004, **233**–**235**; (b) A. G. Craig, O. Roubeau, G. Aromí, *Coord. Chem. Rev.*, 2014, **269**, 13; (c) M. Nihei, T. Shiga, Y. Maedab and H. Oshio, *Coord. Chem. Rev.*, 2007, **251**, 2606; (d) J. A. Real, A. B. Gaspar, V. Niel, and M. C. Munoz, *Coord. Chem. Rev.*, 2003, **236**, 121; (e) M. A. Halcrow, *Chem. Soc. Rev.*, 2011, **40**, 4119.

12 (a) I. Ratera and J, Veciana, *Chem. Soc. Rev.*, 2012, **41**, 303; (b) A. Alberola and M. Pilkington, *Curr. Org. Synth.*, 2009, **6**, 66.

13 (a) A. Caneschi, D. Gatteschi, R. Sessoli and P. Rey, *Accts. Chem. Res.* 1989, **22**, 392; (b) J. D. Rinehart, M. Fang, W. J. Evans, J. R. Long, *Nature Chem.*, 2011, **3**, 538; (c) J. D. Rinehart, M. Fang, W. J. Evans and J. R. Long, *J. Am. Chem. Soc.*, 2011, **133**, 14236.

14 (a) R. M. Buchanan, B. J. Fitzgerald and C. G. Pierpont, *Inorg. Chem.*, 1979, **18**, 3439; (b) H. H. Downs, R. M. Buchanan and C. G. Pierpont, *Inorg. Chem.* 1979, **18**, 1736.

15 A. Caneschi, D. Gatteschi, P. Rey and R. Sessoli, *Inorg. Chem.* 1988, **27**, 1756.

16 (a) D. J. Sullivan, R. Clerac, M. Jennings, A. J. Lough and K. E. Preuss, *Chem. Commun.* 2012, **48**, 10963; (b) K. E. Preuss, *Dalton Trans.* 2007, 2357.

17 (a) R. G. Hicks, M. T. Lemaire, L. K. Thompson and T. M. Barclay, *J. Am. Chem. Soc.*, 2000, **122**, 8077; (b) M. Chahma, K. Macnamara, A. van der Est, A. Alberola, V. Polo and M. Pilkington, *New J. Chem.*, 2007, **31**, 1973; (c) M. Chahma, X.-S. Wang, A. van der Est and M. Pilkington, *J. Org. Chem.*, 2006, **71**, 2750; (d) V. Polo, A

Alberola, J. Andres, J. Anthony and M. Pilkington. *Phys. Chem. Chem. Phys.*, 2008, **10**, 857.
18 W. Fujita and K. Awaga, *J. Am. Chem. Soc*., 2001, **123**, 3601.
19 A.J. Banister, I. May, J.M. Rawson and J.N.B. Smith, *J. Organomet. Chem.*, 1998, **550**, 241; R. T. Boeré, K. H. Moock, V. Klassen, J. Weaver, D. Lentz and H. Michaelschulz, *Can. J. Chem.*, 1995, **73**, 1444.
20 E. R. Clark, J. J. Hayward, B. J. Leontowicz, D. J. Eisler and J. M. Rawson, *Cryst.Eng.Comm.*, 2014, **16**, 1755.
21 (a) J. Zienkiewicz, P. Kaszynski, V. G. Young Jr., *J. Org. Chem.*, 2004, **69**, 2551; (b) J. Zienkiewicz, P. Kaszynski, V. G. Young Jr., *J. Org. Chem.*, 2004, **69**, 7525.
22 (a) E. S. Levchenko, G. S. Borovikova, E. I. Borovik and V. N. Kalinin, *Russ. J. Org. Chem.*, 1984, **20**, 196; (b) D. D. Ross and D. Lednicer, *J. Heterocycl. Chem.*, 1982, **19**, 975; (c) N. Finch, S. Ricca Jr., L. H. Werner and R. Rodebaugh, *J. Org. Chem.*, 1980, **45**, 3416; (d) G. Kresze, C. Seyfried and A. Trede, *Tetrahedron Lett.*, 1965, **44**, 3933.
23 P. G. Welling, *Biopharm. Drug Dispos.*, 1986, **7**, 501; A. Fretheim, *BMC Fam. Pract.*, 2003, **4**, 19.
24 K. S. Hagen, *Inorg. Chem*., 2000, **39**, 5867.
25 PIP Nilges, M, Illinois EPR Research Centre; PIP for windows, *v.1.2* Rawson, J.M. University of Windsor (2011).
26 COLLECT, Nonius (1998), Nonius BV, Delft, The Netherlands.
27 Z. Otwinowski and W. Minor, (1997). Methods in Enzymology, Vol. 276, Macromolecular Crystallography, Part A, (Eds. C. W. Carter Jr and R.M. Sweet) pp. 307-326, Academic Press (New York).
28 A. Altomare, G. Cascarano, C. Giacovazzo, A. Guagliardi, M.C. Burla, G. Polidori and M. Camalli, *J. Appl. Cryst.* 1994, **27**, 435.
29 SHELXTL (2013), Bruker AXS, Madison, Wisconsin, USA
30 APEX, Bruker AXS, Madison, Wisconsin, USA.
31 SAINT, Bruker AXS, Madison, Wisconsin, USA.
32 SADABS, Bruker AXS, Madison, Wisconsin, USA
33 M. J. Frisch, G. W. Trucks, H. B. Schlegel, G. E. Scuseria, M. A. Robb, J. R. Cheeseman, G. Scalmani, V. Barone, B. Mennucci, G. A. Petersson, H. Nakatsuji, M. Caricato, X. Li, H. P. Hratchian, A. F. Izmaylov, J. Bloino, G. Zheng, J. L. Sonnenberg, M. Hada, M. Ehara, K. Toyota, R. Fukuda, J. Hasegawa, M. Ishida, T. Nakajima, Y. Honda, O. Kitao, H. Nakai, T. Vreven, J. J. A. Montgomery, J. E. Peralta, F. Ogliaro, M. Bearpark, J. J. Heyd, E. Brothers, K. N. Kudin,V. N. Staroverov, R. Kobayashi, J. Normand, K. Raghavachari, A. Rendell, J. C. Burant, S. S. Iyengar, J. Tomasi, M. Cossi, N. Rega, J.M. Millam, M. Klene, J. E. Knox, J. B. Cross, V. Bakken, C. Adamo, J. Jaramillo, R. Gomperts, R. E. Stratmann, O. Yazyev, A. J. Austin, R. Cammi, C. Pomelli, J. W. Ochterski, R. L. Martin, K. Morokuma, V. G. Zakrzewski, G. A. Voth, P. Salvador, J. J. Dannenberg, S. Dapprich, A. D. Daniels, Ö. Farkas, J. B. Foresman, J. V. Ortiz, J. Cioslowski and D.J. Fox 7.0 ed.; Wallingford, CT, 2009.
34 (a) P. Hohenberg and W. Kohn, *Phys. Rev.* 1964, **B136**, 864; (b) W. Kohn and L. Sham, *J. Phys. Rev.* 1965, **A140**, 1133; (c) In *The Challenge of d and f Electrons*,; D. R. Salahub and M. C. Zerner Eds.; ACS: Washington, DC, 1989; (d) R. G. Parr and W. Yang, *Density-functional theory of atoms and molecules*; Oxford Univ. Press: Oxford, 1989.
35 (a) A. D. Becke, *J. Chem. Phys*. 1993, **98**, 5648; (b) C. Lee, W. Yang, and R. G. Parr, *Phys. Rev. B* 1988, **37**, 785; (c) B. Miehlich, A. Savin, H. Stoll and H. Preuss, *Chem. Phys. Lett.* 1989, **157**, 200.
36 V. A. Rassolov, J. A. Pople, M. A. Ratner and T. L. Windus, *J. Chem. Phys*. 1998, **109**, 1223.
37 (a) J.S. Binkley, J. A. Pople and W.J. Hehre, *J. Am. Chem. Soc.* 1980, **102**, 939; (b) M. S. Gordon, J. S. Binkley, J. A. Pople, W. J. Pietro and W. J.; Hehre, *J. Am. Chem. Soc.* 1982, **104**, 2797; (c) W. J. Pietro, M. M. Francl, W. J. Hehre, D. J. Defrees, J. A. Pople and J. S. Binkley, *J. Am. Chem. Soc.* 1982, **104**, 5039; (d) K. D. Dobbs and W. J. Hehre, *J. Comput. Chem.* 1986, **7**, 359; (e) K. D. Dobbs and W. J. Hehre, *J. Comput. Chem.* 1987, **8**, 861; (f) K. D. Dobbs and W. J. Hehre, *J. Comput. Chem.* 1987, **8**, 880.
38 (a) W. J. Stevens, W. J. Basch and M. Krauss, *J. Chem. Phys.* 1984, **81**, 6026; (b) W. J. Stevens, M. Krauss, H. Basch, and P. G. Jasien, *Can. J. Chem.* 1992, **70**, 612; (c) T. R. Cundari and W. J. Stevens, *J. Chem. Phys*. 1993, **98**, 5555
39 (a) A. Hauser, *Adv. Polym. Sci.*, 2004, **233**, 49; (b) A.G. Orpen, L. Brammer, H.A. Frank, O. Kennard, D.G. Watson, R. Taylor, *J. Chem. Soc., Dalton Trans.*, 1989, Suppl. **S1** 171; (c) H. Montogomery, R.V. Chastain, J.J. Natt, A.M. Witowsak and E. Lingfelter, *Acta Cryst. E*, 1967, **22**, 775; (d) S. Dick, *Z. Krist*., 1998, **213**, 356
40 D. E. Hamilton, *Inorg. Chem.*, 1991, **30**, 1670.
41 See for example: D. Kivelson and S.-K. Lee, *J. Chem. Phys.*, 1964, **41**, 1896; T.S. Smith II, R. LoBrutto and V.L. Pecoraro, *Coord. Chem. Rev*., 2002, **228**, 1 and refs therein.
42 J. N. B. Smith, J. M. Rawson, and J. E. Davies, *Acta Crystallogr. Sect C*, 1999, **55**, 1330
43 H.F. Lau, V. W. L. Ng, L. L. Koh, G. K. Tan, L. Y. Goh, T. L. Roemmele, S. D. Seagrave and R. T. Boere, *Angew. Chem. Int. Ed. Engl*, 2006, **45**, 4498.

 This journal is © The Royal Society of Chemistry 2014